Reactive Mold Filling in Resin Transfer Molding Processes with Edge Effects

Yanyu Ding,[1] Yuxi Jia,[1] Junying Yang,[2] Sheng Sun,[1] Tongfei Shi,[3] Lijia An[3]

[1]*School of Materials Science and Engineering, Shandong University, Jinan 250061, China*
[2]*School of Materials Science and Engineering, Dalian Jiaotong University, Dalian 116028, China*
[3]*State Key Laboratory of Polymer Physics and Chemistry, Changchun Institute of Applied Chemistry, Chinese Academy of Sciences, Changchun 130022, China*

Received 20 September 2008; accepted 25 February 2009
DOI 10.1002/app.30345
Published online 21 May 2009 in Wiley InterScience (www.interscience.wiley.com).

ABSTRACT: Reactive mold filling is one of the important stages in resin transfer molding processes, in which resin curing and edge effects are important characteristics. On the basis of previous work, volume-averaging momentum equations involving viscous and inertia terms were adopted to describe the resin flow in fiber preform, and modified governing equations derived from the Navier–Stokes equations are introduced to describe the resin flow in the edge channel. A dual-Arrhenius viscosity model is newly introduced to describe the chemorheological behavior of a modified bismaleimide resin. The influence of the curing reaction and processing parameters on the resin flow patterns was investigated. The results indicate that, under constant-flow velocity conditions, the curing reaction caused an obvious increase in the injection pressure and its influencing degree was greater with increasing resin temperature or preform permeability. Both a small change in the resin viscosity and the alteration of the injection flow velocity hardly affected the resin flow front. However, the variation of the preform permeability caused an obvious shape change in the resin flow front. The simulated results were in agreement with the experimental results. This study was helpful for optimizing the reactive mold-filling conditions. © 2009 Wiley Periodicals, Inc. J Appl Polym Sci 113: 3815–3822, 2009

Key words: composites; curing of polymers; reactive processing; rheology; simulations

INTRODUCTION

Resin transfer molding (RTM) is one of the most efficient and attractive techniques for the manufacturing of advanced fiber composites; it is widely used in the automotive and aerospace industries.[1–9] Reactive mold filling is a crucial stage in RTM processes, in which edge effects and resin curing are important characteristics.

In the RTM filling process, small air channels existing between the fiber preform and the mold edge may drastically alter the resin flow patterns; this phenomenon is usually called the *edge effect.* In previous articles on the modeling of the filling process with edge effects, two mathematical models have been proposed. In the first model, the equivalent permeability approach is adopted to simulate the edge flow, and the resin flow in the preform is usually described by means of Darcy's law.[10–14] In the second mathematical model, the Navier–Stokes equations or modified equations derived from the Navier–Stokes equations are introduced into the edge area, and Brinkman–Forchheimer extended Darcy equations or momentum equations considering viscous and inertia effects are used to model the resin flow in the porous medium.[15–17] Obviously, the application of the latter model is wider than that of the former models.

However, in these articles, the resin viscosity was often deemed as a constant, and the influence of the curing reaction on the resin flow fronts and pressures was rarely investigated. In fact, the resin system used in RTM is composed of resin, curing agent, and additives, so the structure and viscosity of the resin system differ with filling time and injection temperature. Particularly for composite parts with high fiber fractions and long resin flow paths, a long mold-filling time is usually consumed, and there often exists a considerable extent of curing reaction; consequently, the effects of the curing reaction on the resin flow fronts and pressures should be considered. In recent years, there has been

Correspondence to: Y. Jia (jia_yuxi@sdu.edu.cn) or L. An (ljan@ciac.jl.cn).

Contract grant sponsor: National Natural Science Foundation of China; contract grant numbers: 50621302 and 20734003.

Contract grant sponsor: Special Funds for National Basic Research Program of China; contract grant number: 2003CB615601.

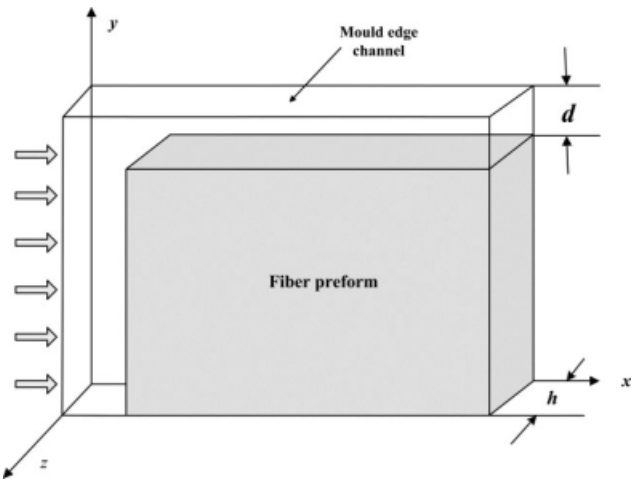

Figure 1 Geometry of the filling model.

notable attention paid to the curing reaction at the mold-filling stage, and a variety of viscosity models have been established.[18–24]

Therefore, on the basis of our previous study,[17] the chemorheological behavior of a modified bismaleimide (BMI) resin at the mold-filling stage is newly described by means of a dual-Arrhenius viscosity model, which was obtained from the experiments by Duan et al.[23] The reactive resin flow process with edge effects was simulated under constant-flow velocity injection conditions, so the influence of the curing reaction and various processing parameters on the resin flow patterns was analyzed.

NUMERICAL PROCESS MODEL

Geometrical model

A geometrical model was constructed in a Cartesian coordinate system, as shown in Figure 1, where d is the distance between the mold wall and the fiber preform and h is the thickness of the mold cavity. The velocity component in the thickness direction was very small, so the resin flow in the cavity was deemed to be a two-dimensional flow.

Mathematical models

Filling in the fiber preform

The fiber preform is a dual-scale porous medium composed of fiber tows and gaps, and the volume-averaging method is widely adopted to obtain modified balance equations.[17,25,26]

The mass conservation equation follows:

$$\frac{\partial\langle u\rangle}{\partial x}+\frac{\partial\langle v\rangle}{\partial y}=0 \tag{1}$$

where $\langle u\rangle$ and $\langle v\rangle$ are the phase-averaged velocity components in the x and y directions, respectively.

When the viscous and inertia effects are considered, the volume-averaging momentum equation is derived as follows:[17,27]

$$\frac{1}{\phi}\frac{\partial(\rho\langle u\rangle)}{\partial t}+\frac{1}{\phi^2}\left[\frac{\partial(\rho\langle u\rangle\langle u\rangle)}{\partial x}+\frac{\partial(\rho\langle u\rangle\langle v\rangle)}{\partial y}\right]=-\frac{\partial\langle p\rangle^f}{\partial x}+\eta_{\text{eff}}\left(\frac{\partial^2\langle u\rangle}{\partial x^2}+\frac{\partial^2\langle u\rangle}{\partial y^2}\right)-\frac{\eta}{K_x}\langle u\rangle \tag{2}$$

$$\frac{1}{\phi}\frac{\partial(\rho\langle v\rangle)}{\partial t}+\frac{1}{\phi^2}\left[\frac{\partial(\rho\langle u\rangle\langle v\rangle)}{\partial x}+\frac{\partial(\rho\langle v\rangle\langle v\rangle)}{\partial y}\right]=-\frac{\partial\langle p\rangle^f}{\partial y}+\eta_{\text{eff}}\left(\frac{\partial^2\langle v\rangle}{\partial x^2}+\frac{\partial^2\langle v\rangle}{\partial y^2}\right)-\frac{\eta}{K_y}\langle v\rangle \tag{3}$$

where ρ is the fluid density; ϕ is the preform porosity; t is the filling time; $\langle p\rangle^f$ is the intrinsic phase-averaged pressure of the fluid; η is the dynamic viscosity; K_x and K_y are the permeabilities of the fiber preform in the x and y directions, respectively; and $\eta_{\text{eff}}=\eta/\phi$ is the effective viscosity.

The simulated domain is discretized into orthogonal grids by means of the finite volume method. For a control volume, ρ and η are calculated from the following formulations:

$$\rho=f\rho_1+(1-f)\rho_2,\quad \eta=f\eta_1+(1-f)\eta_2 \tag{4}$$

where the subscripts denote different fluids, where 1 represents the resin and 2 represents the air, and f is the resin filling fraction in a control volume. If $f(x,y,t)=1$, the control volume is filled with the resin. When $f(x,y,t)=0$, the control volume is full of air or else the air and the resin coexist in the control volume. f can be calculated by the fractional volume function advection equation, which is used to capture the resin flow front and is shown next:[17]

$$\frac{\partial f}{\partial t}+\frac{\langle u\rangle}{\phi}\frac{\partial f}{\partial x}+\frac{\langle v\rangle}{\phi}\frac{\partial f}{\partial y}=0 \tag{5}$$

Flow in the edge area

In the edge area, the resin flow is described by the following equations.

The resin flow is described by the mass conservation equation as follows:

$$\frac{\partial u}{\partial x}+\frac{\partial v}{\partial y}=0 \tag{6}$$

where u and v denote the velocity components in the x and y directions, respectively.

In this study, the x direction was assumed to be the bulk flow direction. The difference between the mold thickness and the edge channel width was too

small to ignore the viscous force in the thickness direction. On the basis of the Navier–Stokes equation, the x-momentum equation in the edge area is modified as follows:[17]

$$\frac{\partial(\rho u)}{\partial t}+\frac{\partial(\rho uu)}{\partial x}+\frac{\partial(\rho vu)}{\partial y}=-\frac{\partial p}{\partial x}+\eta\frac{\partial^2 u}{\partial x^2}-\frac{\eta}{K_{\mathrm{me}}}u \quad (7)$$

where the effect of the mold thickness on the flow pattern is well integrated with the momentum equation by the introduction of the equivalent permeability (K_{me}), which is derived from the following equations:[17,14]

$$K_{\mathrm{me}}=\frac{h^2}{96}\left[1-\frac{192h}{\pi^5 d}\tan h\left(\frac{\pi d}{2h}\right)\right] \text{ when } d\le h \quad (8)$$

$$K_{\mathrm{me}}=\frac{d^2}{96}\left[1-\frac{192d}{\pi^5 h}\tan h\left(\frac{\pi h}{2d}\right)\right] \text{ when } d> h \quad (9)$$

In the y direction, on the basis of the Navier–Stokes equation, the y-momentum equation is simplified as:[17]

$$\frac{\partial(\rho v)}{\partial t}+\frac{\partial(\rho uv)}{\partial x}+\frac{\partial(\rho vv)}{\partial y}=-\frac{\partial p}{\partial y}+\eta\left(\frac{\partial^2 v}{\partial x^2}+\frac{\partial^2 v}{\partial y^2}\right) \quad (10)$$

The fractional volume function advection equation is as follows:

$$\frac{\partial f}{\partial t}+u\frac{\partial f}{\partial x}+v\frac{\partial f}{\partial y}=0 \quad (11)$$

Isothermal chemorheological model

The chemorheological behavior of the resin system during the mold-filling process was newly considered in this study. For a thermosetting resin, the resin viscosity is determined by the shear history, injection temperature, resin reaction kinetics, and filling time.[24] In the RTM filling process, the resin viscosity is not very sensitive to the shear rate; therefore, the resin can be regarded as a Newtonian fluid.[23,28]

In this study, the 6421 resin system, mainly composed of bismaleimidodiphenymethan (BMIM) and allyl bisphenol A and developed by the Beijing Institute of Aeronautical Materials (Beijing, China), was used to infiltrate the preform in the simulation. The reactive groups in this modified BMI resin system mainly undergo homopolymerization, Alder-ene reactions, and copolymerization to form crosslinking structures.[29]

Under isothermal conditions, the chemorheological behavior of the 6421 resin system at the mold-filling stage was investigated experimentally by Duan et al.[23] With increasing filling time, more curing reactions occurred in the resin system, and then, the resin viscosity gradually increased. In addition, the reaction rate increased with increasing temperature, and then, the resin viscosity was more sensitive to the filling time. These evolution laws of resin chemorheological behaviors can be expressed by a dual-Arrhenius viscosity model:[23]

$$\ln\eta(T,t)=-23.996+10,638/T+4.56\times10^7\times t\times\exp(-8971/T) \quad (12)$$

where T is the injection temperature.

With regard to $\eta(x,y,t)$ in a control volume, it can be seen from eq. (4) that it has a close relationship with f. In detail, if $f(x,y,t)=0$, $\eta(x,y,t)$ is the air viscosity. When $0<f(x,y,t)<1$, the resin viscosity in the control volume followed the chemorheological model [eq. (12)], and $\eta(x,y,t)$ was calculated by eq. (4). When $f(x,y,t)=1$, $\eta(x,y,t)$ was equivalent to the resin viscosity; as the case stands, the time in which the resin flowed from the inlet gate to filling up the control volume was fixed, so the resin viscosity and $\eta(x,y,t)$ in the control volume were unchangeable, even when the filling time was increasing.

Hypotheses and boundary conditions

In this study, the fibers were assumed to be rigid, and the inlet flow velocity of the resin was considered to be constant at the mold-filling stage.

The experiments on the resin chemorheological behaviors[23,24,30,31] or on the flow patterns of the RTM processes with edge effects[10,13,14,32,33] were also mostly carried out under isothermal conditions. Therefore, to conveniently select a proper viscosity model fit for the mold-filling process and draw a comparison between the experimental flow patterns and the simulated ones, the isothermal assumption was adopted in this study.

The whole region was considered to be a continuum region, and the single-domain approach was adopted. So the numerical simulation prevented the explicit formulation of the boundary conditions of the edge channel and the fiber preform, and then, the continuity of velocity and normal stress was satisfied spontaneously.

On the mold wall, the method put forward by Salloum et al.[34] was introduced to avoid irrational simulation results. The no-slip boundary condition ($\mathbf{u}=0$, $\mathbf{u}$ is the velocity component in the x direction) and traction free boundary condition ($\mathbf{T}\times\mathbf{n}=0$, where $\mathbf{T}$ is the stress tensor and $\mathbf{n}$ is the unit normal vector) were transformed according to f. In detail, for the mold wall filled with resin, the no-slip boundary condition was adopted. On the contrary, the traction-free boundary condition was applied in the simulation.[17,34,35]

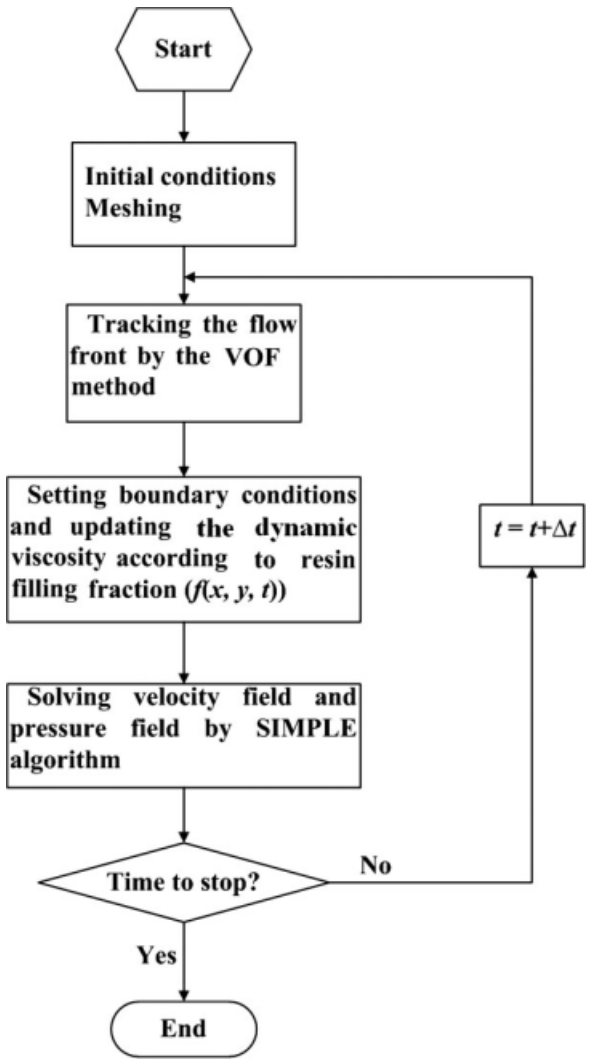

Figure 2 Flow chart of the numerical simulation. The whole filling stage is divided into many time steps, and Δt is the time increment for each time step.

SIMULATION METHODOLOGY AND PROCEDURES

The simulated domain was discretized into orthogonal grids by means of the finite volume method, and the vector variables and the scalar variables were stored separately in the staggered grids. The semi-implicit method for pressure-linked equations (SIMPLE) was introduced to calculate the pressure and the velocity fields.[6,17] To track the resin flow front, the volume of fluid (VOF) method was used.[17,36]

A flow chart of the numerical simulation is illustrated in Figure 2.

RESULTS AND DISCUSSION

The constructed rectangular mold cavity with an edge channel along one side is shown in Figure 1, with dimensions of $0.3 \times 0.09 \times 0.005$ m^3 and a width of edge area of 0.004 m. The other input parameters were as follows: $\rho = 1230$ kg/m^3, air viscosity $= 2.1 \times 10^{-5}$ Pa s, and $\phi = 0.81$.[17]

In the following sections, the model constructed in our study is referred to as the first model, and the existing model from ref. 17 is referred to as the second model. The only difference between the two models is the resin viscosity: in this study, the curing reaction was taken into account, and therefore, the resin viscosity varied with the temperature and the filling time, which followed the chemorheological model. In ref. [17], a constant resin viscosity was adopted, which was equal to the initial value.

It is noteworthy that the pressure referred to in this article is a relative value, which was equal to the difference between the pressure at the inlet gate of the preform and that at the outlet (air pressure).

Effect of the curing reaction on the flow patterns

In this section, the flow patterns simulated by the two models are compared and discussed. The injection conditions were identical for the two models: the resin temperature was 413 K in the filling process, the preform permeability was 2×10^{-9} m^2,[2,17] and the inlet flow velocity of the resin was 0.004 m/s.

With filling times of 25.0, 31.25, and 37.5 s, the shapes and positions of the resin flow fronts obtained from the two models are illustrated in Figure 3. By comparing the simulated results from the first and second models, we found that the occurrence of curing reactions hardly affected the resin flow front in a short filling time. It was because, when the dimensions of the edge channel were unchanged, the shape of resin flow fronts was mainly influenced by the permeability under constant-flow velocity conditions.[32]

To investigate the influence of fluid viscosity on the flow front shape in RTM processes with edge effects, Bickerton and Advani[32] carried out a set of experiments in which the fluid was a mixture of corn syrup, water, and clothing dye. The fluid viscosity was varied in a range, whereas the other processing parameters were maintained constant. The experimental results show that no noticeable effect was found on the flow front shape caused by the viscosity change. Obviously, the characteristics of the simulated results could be validated by the experiments.

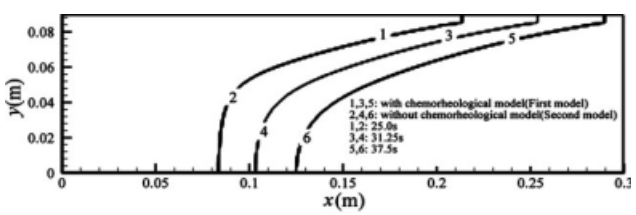

Figure 3 Simulated flow fronts based on the two models.

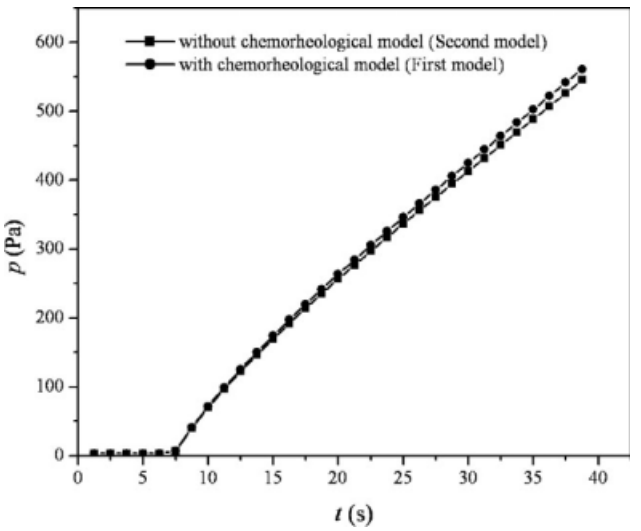

Figure 4 Pressure (p) histories based on the two models.

Although the curing reaction had no obvious effect on the resin flow front in the short filling time, however, as shown in Figure 4, it resulted in an increase of pressure because of the fact that the curing reaction made the resin viscosity increase. As the reaction time increased, more polymerization occurred in the modified BMI resin; then, the average molecular weight of the resin system and the resin viscosity gradually increased. Therefore, the influence of the curing reaction on the pressure was greater.

Effect of the injection temperature on the flow patterns

The injection temperature can influence the initial resin viscosity, the monomer conversion rate, and so on. As the best injection temperature for the 6421 resin system ranged from 403 to 423 K,[23] the injection temperatures adopted in the simulations were 403 and 423 K, respectively. The preform permeability was 2×10^{-9} m^2, and the inlet flow velocity was 0.004 m/s.

As the curing reaction did not pose obvious effects on the resin flow fronts (Fig. 3), the flow fronts simulated by the first model were compared with different injection temperatures, as shown in Figure 5. As expected, when the permeability in the edge channel and that in the preform remained constant, the flow front shape did not change greatly. The small difference, in which the edge flow at 423 K was ahead of the one at 403 K, was caused by the enormous change in the resin viscosity: when the temperature increased from 403 to 423 K, the resin viscosity decreased almost at one order of magnitude. Consequently, a little higher possibility, that the air was trapped inside the fiber preform, may have existed at the higher temperature.

Combining the related simulated results in the Effect of the Curing Reaction on the Flow Patterns section with those in this section, we found that a large variation of the resin viscosity may have caused the small shape changes in the resin flow front, but a small change in the resin viscosity hardly affected the resin flow front. Similar results were also revealed in ref. 6.

The curing reaction influences the pressure, and its influencing degree may be alterable under different processing parameters. In the following sections, a dimensionless variable (p^0), defined as follows, is newly introduced to describe the influencing degree of curing reaction on the pressure. At the same filling time, the pressure difference simulated by means of the two models is divided by the pressure obtained from the first model, as shown next:

$$p^0 = \frac{p_1(t) - p_2(t)}{p_1(t)} \tag{13}$$

where $p_1(t)$ is the pressure simulated in the way of the first model, $p_2(t)$ is the pressure calculated via the second model, and t is the filling time.

A higher value of p^0 indicates that the pressure difference $[p_1(t) - p_2(t)]$ induced by the curing reaction occupies a larger portion of the total pressure, and that the curing reaction results in a greater effect on the pressure.

As shown in Figure 6, when the resin begins to infiltrate the preform, p^0 increases rapidly. At higher injection temperatures, the crosslinking reaction rate is faster, so the resin viscosity is more sensitive to time, which leads to a more obvious effect of resin curing on the pressure and a relatively larger p^0. As the time increases, the difference among p^0 at different temperatures is more distinct.

Higher injection temperatures bring on the better fluidity of the resin system and the decrease of pressure. However, the aforementioned analysis indicated that with increasing temperature, both the discrepancy between the bulk and edge flow and the influencing degree of the curing reaction on the pressure increased. As a result, a proper injection temperature should be chosen, especially for large structural elements that need a long filling time.

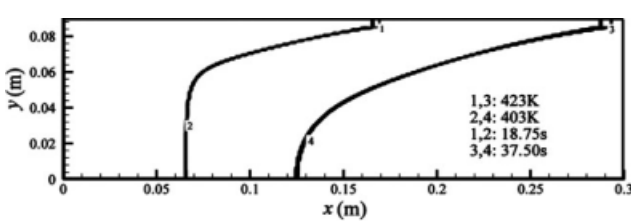

Figure 5 Effect of the injection temperature on the flow front.

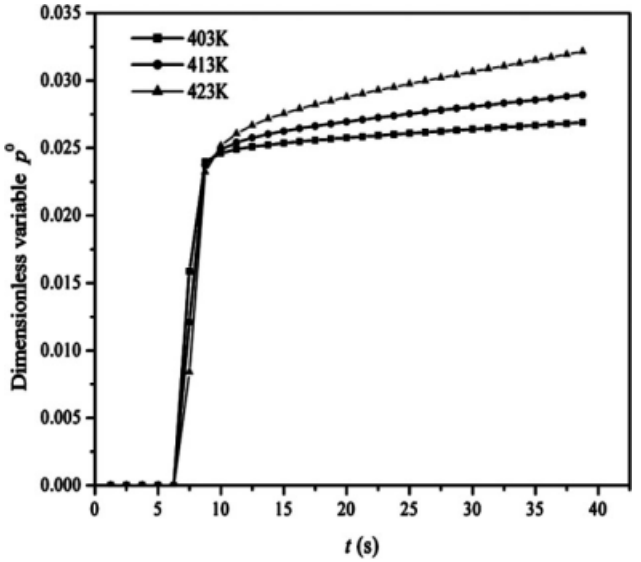

Figure 6 p^0 versus time at different temperatures.

Effect of the flow velocity on the flow patterns

In this part of the study, the resin temperature was kept at 413 K, and the preform permeability was 2 $\times$ 10^{-9} m^2. The flow velocities were chosen to be 0.004 and 0.006 m/s, respectively. As presented in Figure 7, with the same filling fraction, the shapes of the flow front were nearly the same under different flow velocities. This was because, under different flow velocities, the flow resistance in the edge area and that in the preform were the same. In addition, the alteration of the resin viscosity was too small to cause a shape change in the resin flow front. A similar result was also observed in the experiments done by Bickerton and Advani,[32] in which with the injection flow velocity changed, no significant effect on the resin flow front shape was noted.

p^0 was introduced to express the influencing degree of resin curing on the pressure under different flow velocities. When the injection temperature

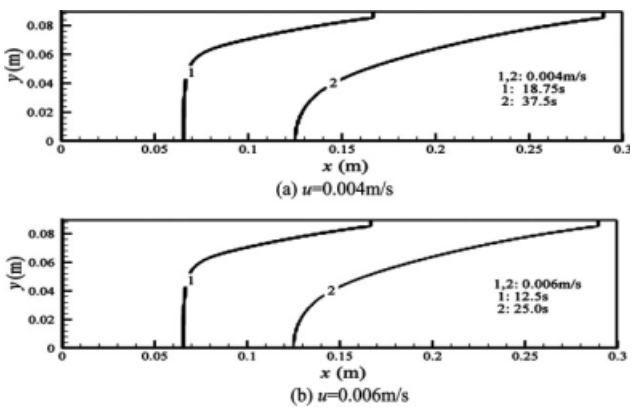

Figure 7 Flow fronts at the same filling fraction under different flow velocities.

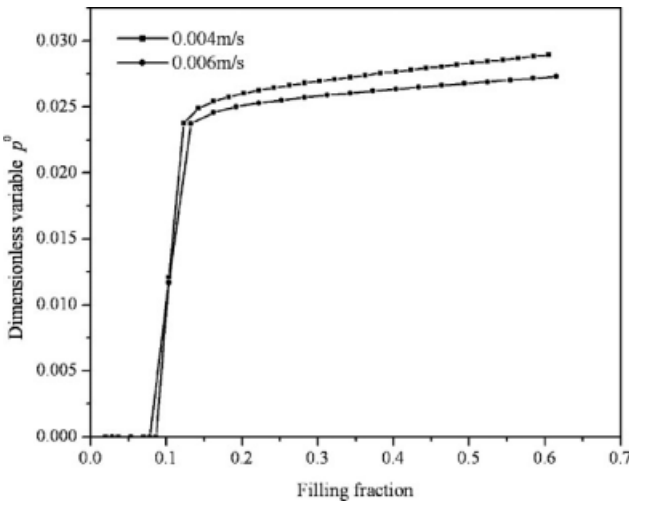

Figure 8 p^0 versus filling fraction at different flow velocities.

and the filling fraction were the same, at a lower flow velocity, more filling time was needed; consequently, the curing degree was greater, and the curing reaction resulted in a more obvious influence on the pressure; correspondingly, p^0 was relatively larger. When the filling fraction increased, the difference between the filling times corresponding to the different flow velocities was more significant; then, the discrepancy of p^0 became more obvious. The results are illustrated in Figure 8.

Effect of the preform permeability on the flow patterns

Preform permeability is a measure of the resistance that the preform poses to the resin flow. To study the influence of preform permeability on the flow patterns, the preform permeabilities applied in the simulation were 2 $\times$ 10^{-9} m^2 (ϕ = 0.81) and 0.97 $\times$ 10^{-9} m^2 (ϕ = 0.685),[37] respectively. The inlet flow

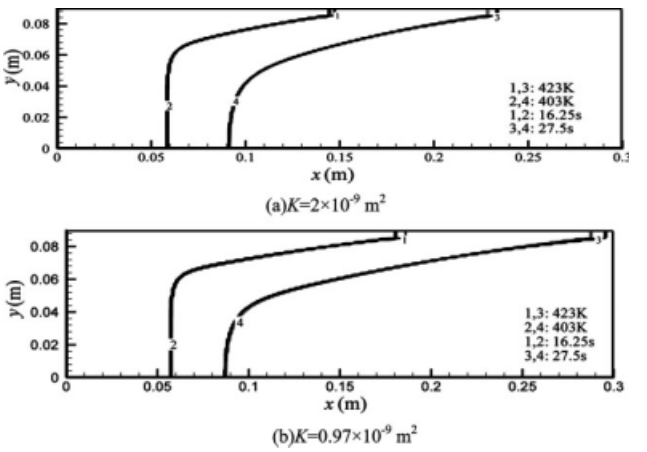

Figure 9 Simulated flow fronts with different preform permeabilities (K's).

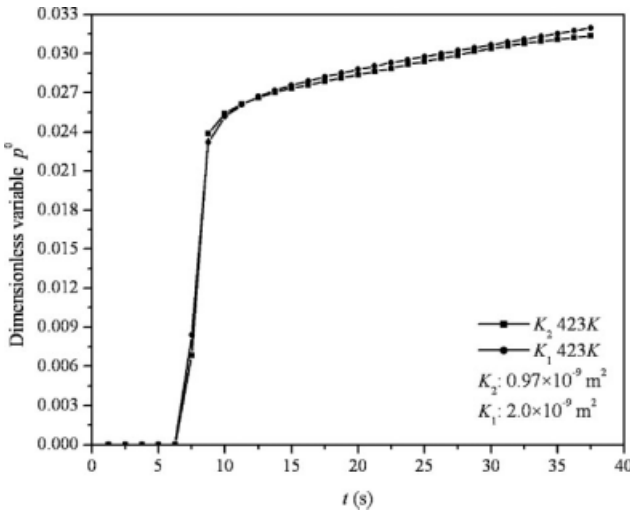

Figure 10 p^0 versus time with different preform permeabilities (K_1 and K_2).

velocity was 0.004 m/s. The resin flow fronts simulated by the first model were compared under different preform permeabilities.

The smaller the preform permeability was, the larger the flow resistance was that existed in the preform, and the transition zone between the bulk flow and the edge flow was greater in the main flow direction, as shown in Figure 9. When the resin viscosity in the same degree decreased (increasing the temperature from 403 to 423 K), the shape change of the resin flow front was a little more obvious under the smaller preform permeability [Fig. 9(b)]. This was because either a drastic decrease in the resin viscosity or a smaller preform permeability made a larger transition zone between the bulk flow and the edge flow in the main flow direction.

When the injection temperature and the filling time were the same, the degree of the curing reaction was the same. However, under the higher preform permeability, f in the preform was larger, and there were more curing reactions occurring in the preform, so the curing reaction resulted in a greater influence on the pressure and p^0 was relatively larger. The previous results are displayed distinctly in Figure 10.

The previous simulated results indicate that, under constant-flow velocity injection conditions, the permeability is one of the most important factors that determine the consistency of the resin flow front in the whole domain. In turn, it affects the formation of dry spots or other defects in the final composite materials.

CONCLUSIONS

Under constant-flow velocity injection conditions, the reactive mold-filling process with edge effects was simulated, and the influences of the curing reaction and various processing parameters on the resin flow patterns were analyzed. The results show that the resin curing reaction caused an increase in the injection pressure and that the influencing degree became greater with increasing resin temperature or preform permeability. No noticeable effect was found on the resin flow front caused by a small change in the resin viscosity or the alteration of the injection flow velocity. However, the permeability was an important factor influencing the resin flow-front shape. Consequently, it affected the possibility that the air was trapped inside the fiber preform and the quality of the composite material. This study was helpful for optimizing the reactive mold-filling conditions.

By comparing these simulated results with the results in published articles, we confirmed the validity of these results. However, nonisothermal conditions may make the reactive mold-filling patterns significantly complicated. On the basis of this study, an investigation involving nonisothermal conditions should be carried out in the future.

References

1. Frederick, R.; Phelan, J. R. Polym Compos 1997, 18, 460.
2. Kuan, Y. D.; EI-Gizawy, A. S. Adv Polym Tech 2000, 19, 173.
3. Akbar, S. Compos A 2006, 37, 1434.
4. Golestanian, H.; EI-Gizawy, A. S. Polym Compos 1998, 19, 395.
5. Ngo, N. D.; Tamma, K. K. Int J Numer Meth Eng 2001, 50, 1559.
6. Yang, J. Y.; Jia, Y. X.; Sun, S.; Ma, D. J.; Shi, T. F.; An, L. J. Mater Sci Eng A 2006, 435-436, 515.
7. Li, J.; Zhang, C.; Liang, R.; Wang, B. Compos A 2005, 36, 564.
8. Simacek, P.; Advani, S. G. Polym Compos 2004, 25, 355.
9. Lawrence, J. M.; Barr, J.; Karmakar, R.; Advani, S. G. Compos A 2004, 35, 1393.
10. Hammami, A.; Gauvin, R.; Trochu, F. Compos A 1998, 29, 603.
11. Hammami, A.; Gauvin, R.; Trochu, F.; Touret, O.; Ferland, P. Appl Compos Mater 1998, 5, 161.
12. Ni, J.; Zhao, Y.; Lee, L. J.; Nakamura, S. Polym Compos 1997, 18, 254.
13. Bickerton, S.; Advani, S. G. Compos Sci Technol 1999, 59, 2215.
14. Young, W. B.; Lai, C. L. Compos A 1997, 28, 817.
15. Costa, V. A. F.; Oliveira, M. S. A.; Sousa, A. C. M. Comput Struct 2004, 82, 1535.
16. Costa, V. A. F.; Oliveira, L. A.; Baliga, B. R.; Sousa, A. C. M. Numer Heat Transfer A 2004, 45, 675.
17. Yang, J. Y.; Jia, Y. X.; Sun, S.; Ma, D. J.; Shi, T. F.; An, L. J. Mater Sci Eng A 2008, 478, 384.
18. Karknas, P. I.; Partrige, I. K. J Appl Polym Sci 2000, 77, 2178.
19. Mijovic, J.; Ott, J. D. J Compos Mater 1989, 23, 163.
20. Lee, C. L.; Wei, K. H. J Appl Polym Sci 2000, 71, 2139.
21. Fontana, Q. P. V. Compos A 1998, 29, 153.
22. Naffakh, M.; Dumon, M.; Gerard, J. F. J Appl Polym Sci 2006, 102, 4228.
23. Shi, F.; Duan, Y. X.; Liang, Z. Y.; Zhang, Z. G. Acta Mater Compos Sinica 2006, 23, 56.
24. Kiuna, N.; Lawrence, C. J.; Fontana, Q. P. V.; Lee, P. D.; Selerland, T.; Spelt, P. D. M. Compos A 2002, 33, 1497.

25. Pillai, K. M. Compos A 2002, 33, 1007.
26. Pillai, K. M.; Munagavalasa, M. S. Compos A 2004, 35, 403.
27. Goyeau, B.; Lhuillier, D.; Gobin, D.; Velarde, M. G. Int J Heat Mass Transfer 2003, 46, 4071.
28. Zhang, Z. G.; Zhamu, A.; Ren, Q.; Chen, C. Acta Aeronautica Astronautica Sinica 2004, 25, 312.
29. Zhuang, H. Ph.D. dissertation, Virginia Polytechnic Institute and State University, 1998.
30. Xiong, Y.; Boey, F. Y. C.; Rath, S. K. J Appl Polym Sci 2003, 90, 2229.
31. Boey, F. Y. C.; Song, X. L.; Yue, C. Y.; Zhao, Q. J Polym Sci Part A: Polym Chem 2000, 38, 907.
32. Bickerton, S.; Advani, S. G. In Recent Advances in Composite Materials; White, S. R.; Hahn, H. T.; Jones, W. F., Eds.; American Society of Mechanical Engineers: New York, 1995.
33. Mohan, R. V.; Shires, D. R.; Tamma, K. K.; Ngo, N. D. Polym Compos 1998, 19, 527.
34. Hétu, J. F.; Gao, D. M.; Garcia-Rejon, A.; Salloum, G. Polym Eng Sci 1998, 38, 223.
35. Chang, R. Y.; Yang, W. H. Int J Numer Meth Fl 2001, 37, 125.
36. Gueyffier, D.; Li, J.; Nadim, A.; Scardovelli, R.; Zaleski, S. J Comput Phys 1999, 152, 423.
37. Hu, X. B.; Ma, Y. L.; Wang, Z. D.; Wu, D. D. Fiber Reinforced Plast/Compos 1996, 3, 25.